Synthesis of NiO/YSZ Nanocomposite Particles using Co-precipitation Method

SATO Kazuyoshi[*] and OHARA Satoshi[**]

Abstract

NiO/Yttria-stabilized zirconia (YSZ) composite particles were synthesized via a co-precipitation of hydroxides. The effect of precipitation and agglomeration behaviors of the hydroxides in an aqueous solution on the morphology of the composite particles was investigated by varying pH from 11 to 13. The particles synthesized at pH 12, or lower, involved large angular NiO particles with the size > 1μm due to slower precipitation or agglomeration of Ni(OH)$_2$, while NiO/YSZ nanocomposite particles with the primary particle size of < 100 nm were obtained at pH 13. This can be attributed to rapid precipitation as well as better dispersion of the hydroxides in the aqueous solution.

KEY WORDS: (Solid oxide fuel cells) (Ni/YSZ anode) (NiO/YSZ) (Composite particles) (Co-precipitation)

1. Introduction

Nickel/yttria stabilized zirconia (Ni/YSZ) cermet is a promising anode material for solid oxide fuel cells (SOFCs). Since their electrochemical performance strongly depends on the microstructure, [1,2] considerable efforts have been made for the precise control of the microstructure.[3-5] Previous fundamental studies revealed that an electrochemical reaction, hydrogen oxidation occurs at the triple phase boundary (TPB) where Ni, YSZ and pore phases meet.[6,7] Detailed electrochemical investigations indicated that the dominant rate limiting steps involved dissociative adsorption of hydrogen molecules onto the anode surface, diffusion of the hydrogen atoms on the surface moving toward the TPB, and a charge transfer reaction at the TPB. [8,9] A finer microstructure consisting of uniformly arranged Ni, YSZ and pore phases would reduce the contribution of these steps, resulting in better electrochemical performance.

Prefabrication of NiO/YSZ composite particles and their three dimensional assembly is a promising route for precise control of the anode microstructure.[10-12] A variety of methods such as spray pyrolysis,[10] mechanical milling,[11] gel combustion [12] had been proposed to synthesize these composite particles.

Co-precipitation is one of the most widely used methods to produce various nanoparticles in industry, since the method can provide them at relatively low cost. There are some challenges for the synthesis of NiO/YSZ composite particles with the method.[13-15] However the grain size was around 1 μm or more in state-of-the-art Ni/YSZ anode derived from the composite particles. This may be due to the lack of precision of the control of

synthesis parameters. Recently, we found that NiO/YSZ nanocomposite particles can be synthesized when the hydroxide precursor was co-precipitated at pH 13.[16] The anode derived from the composite particles had uniform porous structure consisted of fine grains in the range 200-400 nm, and demonstrated good electrochemical performance. It is necessary to understand the formation mechanism of the NiO/YSZ nanocomposite particles for further high performance of the anode.

The present study aimed to understand the effect of precipitation and agglomeration behavior of the hydroxide precursors on the morphology of the NiO/YSZ composite particles.

2. Solubility curves of the hydroxides

It is of primary importance to understand the precipitation behavior of the precursor for precise morphology control of the composite particles. The precipitation of metal hydroxide M(OH)$_n$ can be described as,

$$M^{n+} + n(OH)^- \rightarrow M(OH)_n \tag{1}$$
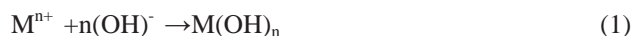
where n is the valence of metal ions in the solution. The solubility product K_{SP} of M(OH)$_n$ is

$$K_{SP} = [M^{n+}][OH^-]^n \tag{2}$$
$$\log K_{SP} = \log[M^{n+}] + n \cdot \log[OH^-] \tag{3}$$

[M^{n+}] and [OH$^-$] were the mole concentrations of M^{n+} and OH$^-$ in the solution, respectively. The ionic product of water at 25 ºC under the ambient pressure was 10^{-14} M^2.

-log $[H^+]$-log $[OH^-]$=pH+pOH=14   (4)

Therefore eq. (3) can be described as follows.

$\log K_{SP}=\log[M^{n+}]-14n-$ n·$\log[H^+]$ (5)
$\log[M^{n+}]=-\log K_{SP}+14n-$ n·pH   (6)

log K_{SP} can be found in the literature.[17, 18] **Figure 1** shows the solubility curves of $Zr(OH)_4$, $Y(OH)_3$ and $Ni(OH)_2$ as a function of pH. This figure indicated that $Zr(OH)_4$ starts to precipitate prior to $Y(OH)_3$ and $Ni(OH)_2$, and is almost finished at pH 4, then other hydroxides start to precipitate. Thus it would be difficult to synthesize homogeneous NiO/YSZ composite particles using a conventional co-precipitation condition, in which the pH of the solution containing constituent metal ions was increased step by step by adding some basic solution. To minimize the inhomogeneous precipitation, the pH of the solution should be high enough and kept constant during the precipitation.

3. Experimental procedure

Figure 2 shows synthesis procedure for NiO/YSZ composite particles. All the reagents were purchased from Kanto Chemical. Co. Ltd, Japan. $ZrOCl_2 \cdot 8H_2O$, $Y(NO_3)_3 \cdot 6H_2O$ and $Ni(NO_3)_2 \cdot 6H_2O$ were dissolved into deionized water to prepare the source solution with the total metal ion concentration of 0.2 M. The solution was added dropwise into the concentrated NaOH solution to precipitates the hydroxides. During the precipitation, extra NaOH solution was added simultaneously to keep pH constant (pH11, 12 or 13). The precipitates were washed by water four times and by ethanol once, and then dried in an oven at 80 °C for 24 h. After pulverization using an alumina mortar and pestle, the precursors were
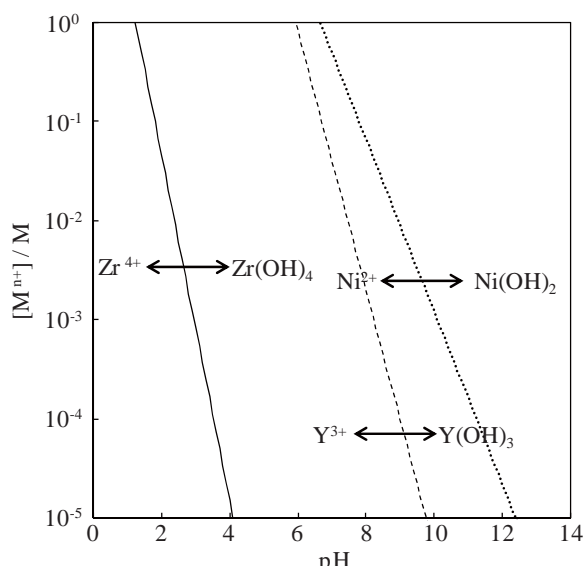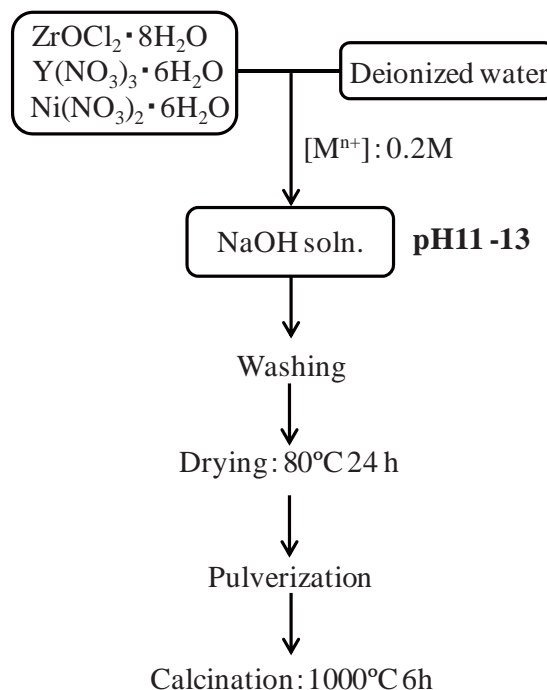

Fig. 2 Scheme of the synthesis of NiO/YSZ composite particles.

calcined at 1000 ºC for 6 h to convert them into NiO/YSZ composite particles. Morphology of the composite particles was characterized by scanning electron microscopy (SEM; ERA-8800FE, Eloinics, Japan) with energy dispersive X-ray spectroscopy (EDS).

4. Results and discussion

Figure 3 shows SEM micrographs of NiO/YSZ composite particles synthesized at different pH levels. The composite particles synthesized at pH 11 and pH 12 consisted of large angular particles and agglomerated fine particles. The analysis by EDS revealed that the former were NiO and the later were NiO/YSZ composites, respectively. Homogeneous composite particles consisting of nano-sized particles were obtained at pH13 (see inset of Fig. 3 (c)).

Although, particle size was expected to decrease monotonically with increasing pH from the consideration of nucleation density, the size of coarse NiO discontinuously changed with respect to pH. The fact suggested that there are other factors affecting the morphological evolution of the composite particles in addition to the precipitation behavior. Agglomeration behavior of the hydroxides would be a possible factor.

Figure 4 shows zeta potential curves of the hydroxide. The curves represent charging state of the hydroxide surfaces in the aqueous medium with various pH levels. $Zr(OH)_4$ had negative charge in the present pH range. While $Ni(OH)_2$ had positive charge at pH11, almost zero at pH 12, and negative at pH 13. Furthermore, $Y(OH)_3$ had a positive charge at pH 11 and negative above pH 12.
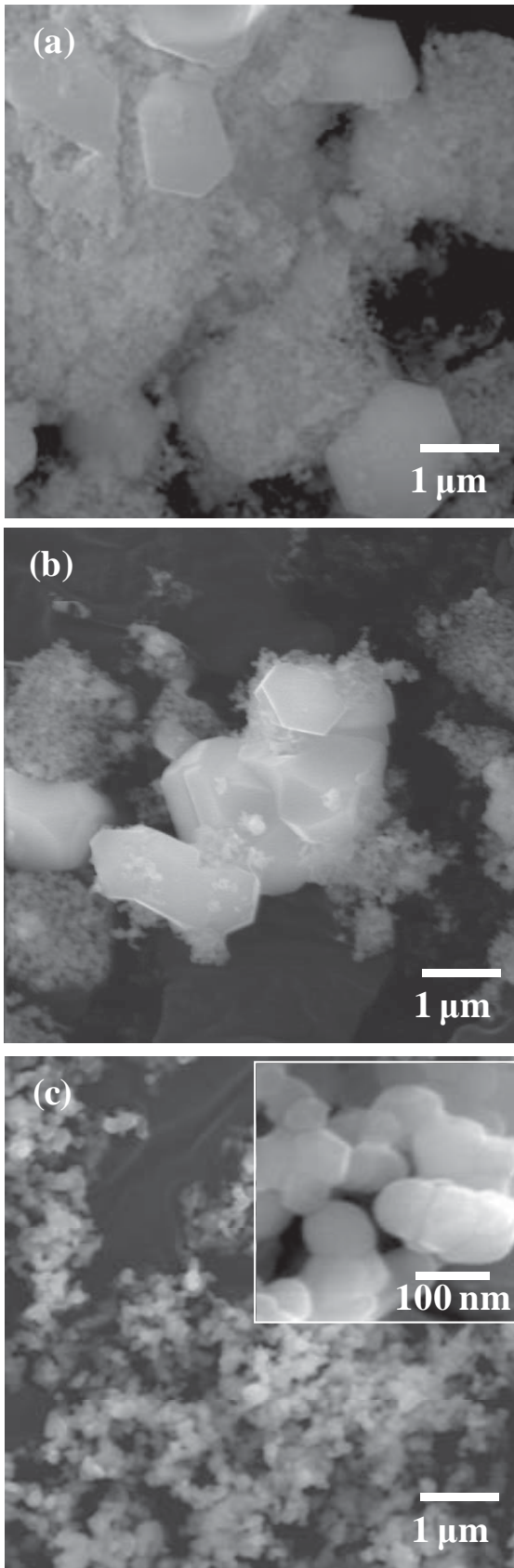

Fig. 1 Solubility curves of $Zr(OH)_4$, $Y(OH)_3$ and $Ni(OH)_2$ at 25 ºC.

Fig. 3 SEM micrographs of the NiO/YSZ composite particles synthesized at (a) pH 11, (b) pH 12 and (c) pH13.
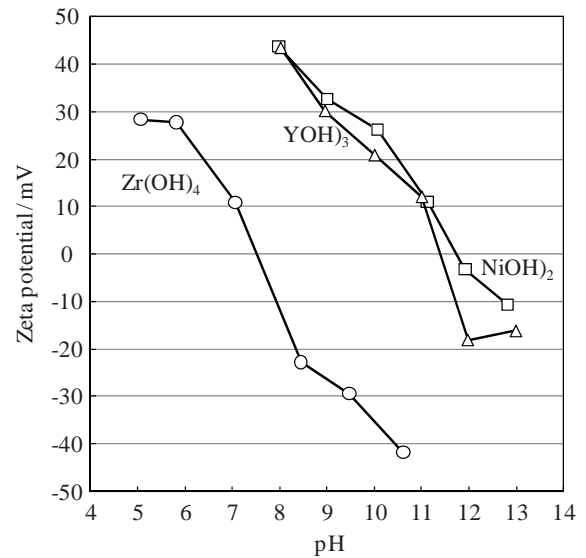

Fig. 4 Zeta-potential curves of $Zr(OH)_4$, $Y(OH)_3$ and $Ni(OH)_2$

The following is possible evolution mechanisms of the composite microstructure. Electrostatic coagulation would occur between $Zr(OH)_4$ and oppositely charged $Ni(OH)_2$ and $Y(OH)_3$ at pH 11, however part of the $Ni(OH)_2$ precipitated after the coagulation due to the slower dehydration of Ni^{2+}, forming agglomerated regions of $Ni(OH)_2$. The agglomerated $Ni(OH)_2$ transformed into NiO with significant grain growth during the calcination, resulting in large angular particles.

Negatively charged $Zr(OH)_4$ and $Y(OH)_3$ would be dispersed uniformly without forming agglomerates in the solution at pH 12. While $Ni(OH)_2$ would form larger agglomerates than the case of pH11, since their surface charge was almost zero, in which electrostatic repulsion force did not work well. The larger agglomerates would be converted into aggregated angular NiO particles as shown in Fig. 3 (b).

Rapid precipitation would result finer hydroxides at pH 13. In addition, all of $Zr(OH)_4$, $Y(OH)_3$ and $Ni(OH)_2$ had negative charges, which suppressed their agglomeration electrostatically. As a consequence, the precursor consisting of uniformly distributed finer $Zr(OH)_4$, $Y(OH)_3$ and $Ni(OH)_2$ was obtained. The uniformly distributed phases suppressed each other's grain growth during the subsequent calcination step,[11] resulting in homogeneous NiO/YSZ nanocomposite particles as shown in Fig.3 (c).

5. Conclusions

Precipitation and agglomeration behavior of the hydroxide precursors depending on pH, strongly affected the morphology of the NiO/YSZ composite particles. Both rapid precipitation and better dispersion of each hydroxide in the solution are necessary to fabricate nanosized NiO/YSZ composite particles through this method. These conditions were fulfilled above pH 13.

References

1) M. Brown, S. Primdahl, M. Mogensen, J. Electrochem. Soc., 147 (2000) 475-485.

2) S. Primdahl, M. Mogensen, J. Electrochem. Soc., 144 (1997) 3409-3419.

3) T. Kawada, N. Sakai, H. Yokokawa, M. Dokiya, M. Mori, T. Iwata, J. Electrochem. Soc., 137 (1990) 3042-3047.

4) S. P. Jiang, Y. Y. Duan, J. G. Love, J. Electrochem. Soc., 149 (2002) A1175-A1183.

5) S. P. Jiang, S. Zhang, Y. D. Zhen, W. Wang, J. Am. Ceram. Soc., 88 (2005) 1779-1785.

6) J. Mizusaki, H. Tagawa, T. Saito, K. Kamitani, T. Takagi, T. Hikita, M. Ippommatsu, S. Nakagawa, K. Hasgimoto, J. Electrochem. Soc., 141 (1994) 2129-2134.

7) A. Bieberle, L. P. Meier, L. J. Gauckler, J. Electrochem. Soc., 148 (2001) A646-A656.

8) S. P. Jiang, S. P. S. Badwal, J. Electrochem. Soc., 144 (1997) 3777-3784.

9) S. P. Jiang, Y. Ramprakash, Solid State Ionics, 122 (1999) 211-222.

10) T. Fukui, S. Ohara, M. Naito, K. Nogi, J. Power Sources, 110 (2002) 91-95.

11) T. Fukui, K. Murata, S. Ohara, H. Abe, M. Naito, K. Nogi, J. Power Sources, 125 (2004) 17-21.

12) S.-D. Kim, H. Moon, S.-H. Hyun, J. Moon, J. Kim, H.- W. Lee, J. Power Sources, 163 (2006) 392-397.

13) S. Mosch, N. Trofimenko, M. Kusnezoff, T. Betz M. Kellner, Solid State Ionics, 179 (2008) 1606-1610.

14) M. Marinšek, K. Zupan, J. Maček, J. Power Sources, 86 (2000) 383-389.

15) C. M. Grgicak, R. G. Green, W.-F. Du , J. B. Giorgi, J. Am. Ceram. Soc., 88 (2005) 3081-3087.

16) K. Sato, G. Okamoto, M. Naito, H. Abe, J. Power Sources, 193 (2009) 185-188.

17) L. G. Sillén, A. E. Martell, Stability Constants of Metal-Ion Complexes, Chemical Society, London. No. 17 (1964) and No. 25 (1971).

18) W. Feitknecht, P. Scindler, Pure Appl. Chem., 6 (1963) 130-199.